Maximum power point tracking and space vector modulation control of quasi-z-source inverter for grid-connected photovoltaic systems

Essaid Jaoide[1], Faicel El Aamri[2], Mbarek Outazkrit[1], Abdelhadi Radouane[1], Azeddine Mouhsen[1]

[1]Laboratory of Radiation-Matter and Instrumentation, Faculty of Science and Technology, University Hassan 1st, Settat, Morocco
[2]Laboratory of Materials Energy and System Control, Faculty of Science and Technology, Hassan II University, Mohammedia, Morocco

ABSTRACT

The quasi-Z-source inverter (qZSI) become one of the most promising power electronic converters for photovoltaic (PV) applications, due to its capability to perform a buck-boost conversion of the input voltage in a single stage. The control strategy based maximum power point tracking (MPPT) and proportional integral (PI) controller are well known in grid-connected with traditional configuration but not in qZSI. This paper presents a control strategy for qZSI grid-connected based on the MPPT algorithm and the linear control by PI controllers. This is complemented by the capability to efficiently transfer the harvested power to the grid, ensuring a unity power factor. The proposed control strategy effectively separates the control mechanisms for the direct current (DC) and alternating current (AC) sides by utilizing the two control variables, the shoot-through duty ratio and the modulation index. An adapted space vector modulation technique is then utilized to generate the switching pulse width modulation (PWM) signals, using these two control variables as inputs. The proposed approach was tested and validated under MATLAB/Simulink and PLECS software.

This is an open access article under the CC BY-SA license.

Corresponding Author:

Essaid Jaoide
Laboratory of Radiation-Matter and Instrumentation, Faculty of Science and Technology, University Hassan 1st
Settat, Morocco
Email: e.jaoide@uhp.ac.ma

1. INTRODUCTION

The substantial rise in energy requirements and the rapid depletion of fossil fuel reserves globally has led to an increase in energy prices, as well as concerns regarding energy security and environmental impacts. In this context, photovoltaic (PV) systems offer a clean and reliable alternative for the generation of green energy. Indeed, the PV energy is rapidly becoming an essential component of power systems. The use of PV systems has been historically confined to standalone configurations in a variety of applications. However, the remarkable decrease in the cost of PV modules, the implementation of PV systems has expanded beyond standalone configurations to include integration with grid-connected systems [1]. Over the past decade, both government entities and private sectors have incentivized the power industry to embrace the integration of PV solar energy into medium or low-voltage distribution grids, owing to the decline in cost of power electronic devices and advancements in renewable energy technology.

As the utilization of solar PV systems continues to increase, it is imperative to examine and understand the challenges that arise during the extraction of energy from these systems and its subsequent integration into the electrical grid. In addition, the generation of solar PV energy requires processing through a power electronics interface before it may be used. To address the issue of lower input voltage caused by

constraints in the PV strings connection, an inverter system applied with the PV source often incorporates a DC-DC boost converter. This one is inserted in between to increase the voltage at the inverter's DC-link, enabling the connection to the grid and facilitating the maximum power point tracking (MPPT) operation [2]–[5]. This additional stage leads to an increased volume and supplementary losses, consequently ending with a decrease in the overall system efficiency [1], [2].

To overcome these limitations of dual stage conversion, the Z-source inverter (ZSI) has been proposed [6]. In fact, the ZSI exhibits a distinctive configuration that enables it to achieve a significant voltage buck-boost capability within a single stage. That is to say, providing an efficient means to manage energy transfer between a power supply and a grid [2], [6].

Following the introduction of ZSI topology, a number of daughters topologies were subsequently developed to enhance the inherent capabilities of the original topology [7], [8]. In the same hand, the most promising topology is the quasi-Z source inverter (qZSI) which was introduced in 2008, due to its ability to harvest the maximum power for PV systems [9]. In various research studies, the qZSI has been utilized in conjunction with renewable energy sources, including PV systems [10], [11] and wind turbines [12].

The qZSI uses an L-C impedance network as shown in Figure 1, it allows the use of an extra-state named the shoot-through (ST) state which is the mechanism used to boost the input voltage [2], [6]. Moreover, the implementation of the ST state can be achieved by simultaneous switching of the upper and lower devices within a single phase-leg of the qZSI.

Three-phase qZSI have the capability to employ various conventional pulse width modulation schemes or space vector modulation (SVM) schemes. However, it should be noted that the utilization of the ST state cannot be feasible without adapting these methods to adhere to the operational principles of the qZSI. In this context, many pulse width modulation (PWM) control methods tailored for qZSI have been proposed in the literature [13]–[15].

The main objective of grid-connected PV applications is to invert the direct current (DC) power generated by the PV generator into alternating current (AC) power that can be transmitted to the grid [1]. In the case where a fixed topology is chosen for the grid-connected inverter, the control strategy plays a crucial role in determining the overall performance of the system [1]. A well-designed control strategy can significantly enhance the power quality of the grid-connected inverter and improving its overall effectiveness. Therefore, the design of the control box claims to obtain the optimal power output from the PV panels while maintaining the required power factor and minimizing the output total harmonic distortion (THD). In order to achieve an effective qZSI performance control strategy, it is essential to develop a precise dynamic model of the system. Various mathematical models were introduced in the literature to analyze and optimize the performance of the overall system [2], [16]–[18]. Also, the feedback control strategies for qZSI have been the subject of investigation in several recent scholarly works [17], [19]–[24].

Currently, the control methods employed for qZSI mainly comprise proportional integral [2], [11], [12], proportional resonance control [17], [25], sliding mode control [21], predictive control [24], and various other techniques [22], [23]. Based on the analysis of the existing literature, it can be inferred that the non-linear control methods demonstrate superior dynamic response compared to proportional integral (PI) controllers [2], [8]. Nevertheless, the complexity associated with these algorithms prevents their widespread implementation, which encourage the need for continued exploration and investigation into linear control approaches.

In this regard, for the linear control of qZSI for PV application, many closed-loop control schemes have been reported in the literature to effectively regulate the DC-link voltage. Notable examples included direct DC-link control, indirect DC-link control, dual-loop controls and unified control. These schemes control have been widely studied and used to achieve accurate and reliable DC-link voltage control [8].

Associated with PV generator, several research works have shown that the qZSI inverter is able to handle variations of the PV output voltage and to produce an output voltage adapted to the grid-connected [2], [8], [10], [19], [26]. The studies reported in [10], [11], [22], [27] employs the MPPT algorithm to generate the ST duty ratio, while the reference d-axis current on the grid side is obtained through the control loop of the impedance network capacitor voltage. Other studies such as [12], [16], [24], [26] use the MPPT algorithm to generate the d-axis current reference of the grid.

The principal objective of this work was to achieve the optimal utilization of power generated by PV panels with employing a linear control strategy based on the MPPT algorithm and the PI-ZSVM (SVM adapted to qZSI) technique. This paper exclusively focuses on the discussion of the grid-connected mode for the qZSI, while the examination of standalone mode has been addressed in previous studies [28]. On the other hand, it introduces a strategy for controlling separately both DC-link voltage and the AC-side current. In the proposed control scheme, the peak DC-link voltage is indirectly estimated by considering the voltage across the capacitors of the qZSI, the ST duty ratio is generated through a double loop control according to the error signal of the DC-link voltage. Furthermore, the AC-side control ensures synchronization of injected current and controls power transfer quality. The amplitude of the d-axis grid current reference is elaborated

through a PI controller in accordance with the error signal of the MPPT algorithm. The proposed control scheme is simulated on the PLECS software and MATLAB/Simulink environment. Hence, the obtained results show the effectiveness of the control scheme and controller proposed and examined in this work.

The present paper is organized as follows: the section 2 provides a comprehensive explanation of the distinct elements comprising the control strategy proposed. Specifically, we have provided detailed descriptions of the qZSI and its dynamic modeling, the adapted MPPT algorithm, grid synchronization, the ZSVM technique, and the multiple control loops employed within the proposed control scheme. In section 3, the simulation results are depicted and discussed. Finally, the conclusion and the perspectives of this work is reported in section 4.
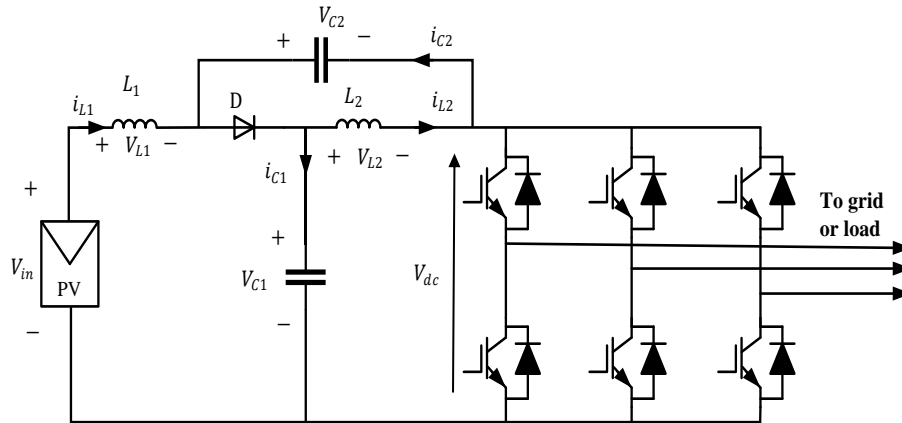
Figure 1. qZSI inverter structure

2. METHOD
2.1. qZSI modelling

The PV generator typically necessitates a two-stage power converter [2]–[5], which uses a DC-DC boost converter and a bidirectional two-level voltage-source inverter (VSI) to regulate DC-link voltage, so as to the power flow between the PV generator and the grid. This topology suffers from several constraints, notably the decrease in its efficiency and the high cost [2], [7].

In this present study, the conventional two-stage power converter is substituted with a qZSI, which comprises an impedance network and a two level VSI. Through the implementation of an efficient switching control, the qZSI allows regulation of the active and reactive power exchanged with the grid, as well as the DC-link voltage. Figure 2 presents the equivalent circuit of qZSI in its two operating states. The operating principle of qZSI is based on an extra-state called shoot-through state. During this one, at least one arm of the inverter is short-circuited. In fact, Figure 2(a) shows the equivalent circuit of the qZSI during this state. Out of the shoot-through sequence, the qZSI works as a traditional inverter, the energy transfer is done towards the load or the grid. The equivalent circuit of the qZSI during this state is shown in Figure 2(b). Note that the shoot-through sequence does not affect the proper operation of the grid or the load.

(a)	(b)
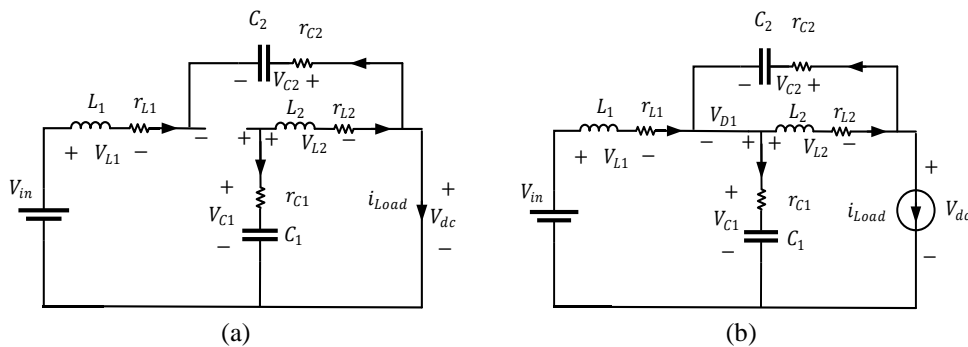
Figure 2. Equivalent circuit of qZSI, (a) in shoot-through state and (b) in non-shoot-through state

Henceforth, we shall adopt the nomenclature of the currents and voltages depicted in Figure 1 for all subsequent analyses. We will also designate by: T_C is switching cycle, T_S is interval of the ST state, T_{NS} is interval of the NST state, $D = \frac{T_S}{T_C}$ is shoot-through duty ratio. During shoot-through interval, we can write:

$$V_{dc} = 0, v_{L1} = V_{C2} + V_{in}, v_{L2} = V_{C1} \tag{1}$$

At the non-shoot-through interval, we have:

$$V_{dc} = V_{C1} + V_{C2}, v_{L1} = V_{in} - V_{C1}, v_{L2} = -V_{C2} \tag{2}$$

During a single switching cycle in steady state, the mean voltage across the inductors is zero. Therefore, using (1) and (2), we obtain:

$$V_{L1} = \overline{v}_{L1} = D(V_{C2} + V_{in}) + (1 - D)(V_{C1} - V_{in}) = 0 \tag{3}$$

$$V_{L2} = \overline{v}_{L2} = DV_{C1} + (1 - D)(-V_{C2}) = 0 \tag{4}$$

Consequently, we can infer the subsequent expressions:

$$V_{C1} = \frac{1-D}{1-2D}V_{in} \text{ and } V_{C2} = \frac{D}{1-2D}V_{in} \tag{5}$$

The peak input voltage of the inverter V_{dc} in the active state can be expressed as (6).

$$V_{dc} = V_{C1} + V_{C2} = \frac{1}{1-2D}V_{in} = BV_{in} \tag{6}$$

Here, *B* represents the boost factor of the qZSI. In theory, the gain factor can be varied from one to infinity by changing the duty cycle (D) between 0 and 0.5. But in practical situations, this factor is restricted by external factors related to the modulation index of the AC side [2], [6], [9].

2.2. Proposed control strategy of qZSI PV grid-connected

The proposed structure of the qZSI PV grid-connected is illustrated in Figure 3. This one shows the different components of the system and how they are interconnected. The role of the section is to provide a detailed description of the various components comprising the proposed control scheme.
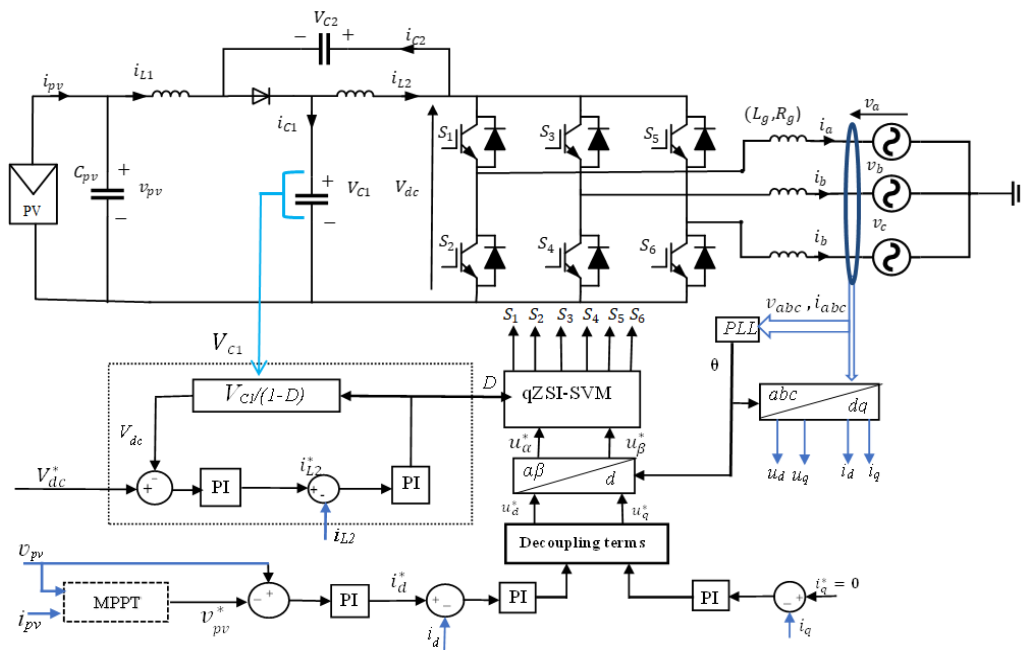
Figure 3. Structure and scheme control proposed for qZSI and PV grid-connected

2.2.1. MPPT algorithm

PV array characteristic is non-linear, which is why there is a maximum power point (MPP), and it depends on environmental conditions. So, the operating point needs to be updated to follow weather conditions. The mathematical model describing the PV modules can be referred to in [5]. The P-V curve of the PV panel, as depicted in Figure 4, clearly illustrates that the output power is maximized at a single operating terminal voltage, denoted as V_{mpp}, which corresponds to the MPP.

The MPPT algorithm was proposed to keep the operating point at MPP in all conditions. In this context, several MPPT techniques have been presented in the literature to optimize the power production of PV systems [29]. Moreover, it is widely recognized that the basic P&O (perturb and observe) algorithm is the most efficient under normal operating conditions.

The P&O MPPT algorithm operates by analyzing the derivative of both the PV generator power and voltage, represented by $\frac{dP}{dV}$. To gain a clearer insight, Figure 5 displays the flowchart depicting the MPPT P&O algorithm used in the proposed control scheme. The MPPT control involves the measurement of PV voltage and current, which are subsequently fed as inputs to the MPPT block. The P&O algorithm generates the PV voltage reference, which is refreshed periodically.
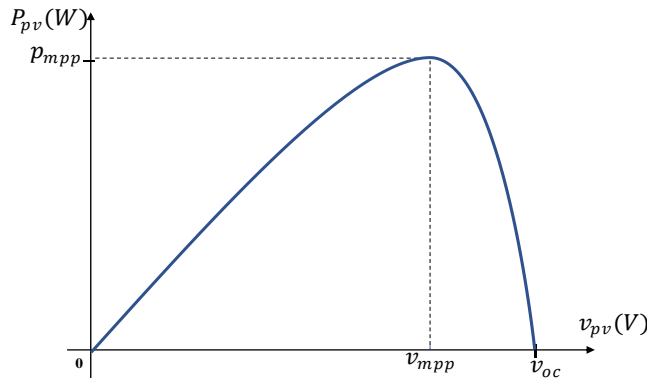
Figure 4. Example of P-V characteristics of the PV panel
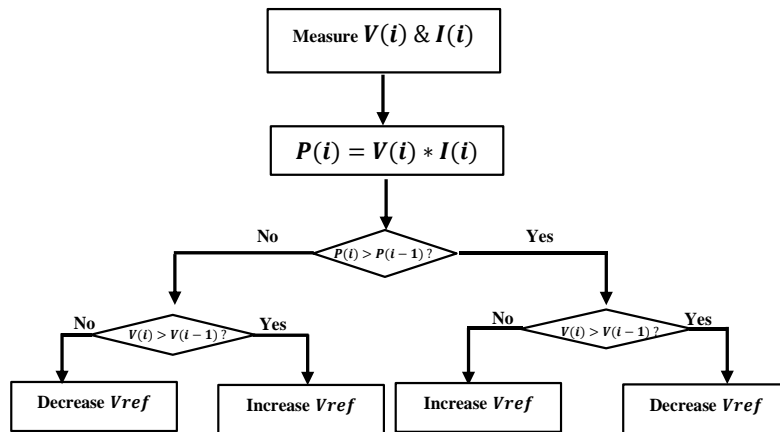
Figure 5. The flowchart of the MPPT P&O algorithm used for qZSI

2.2.2. Grid synchronization

Grid synchronization is an adaptive process in which the control algorithm of the grid-connected converter generates a specific grid variable, typically the fundamental component of the grid voltage. This adaptive process is essential for ensuring the stable and reliable operation of grid-connected power converters, which are critical components of modern power systems. The synchronization process allows to know the phase angle of the grid voltage, and it is used to regulate the active and reactive power supplied by a power converter connected to the grid.

Synchronous reference frame phase locked loop (PLL) is used in this work, due to its simple implementation and ability to estimate quickly and accurately the phase/frequency in normal grid condition [30]. Initially, the sensed grid phase voltages v_{gabc} are converted into the synchronous d-q frame. Then, the PI controller is subsequently employed to regulate the q variable, with the output of this PI serving as the grid frequency. The utility phase angle is derived by integrating the aforementioned grid frequency [30].

2.2.3. ZSVM control technique

In contrast to the conventional VSI, which does not permit the existence of the ST state, qZSI allows this state by utilizing an impedance network. The ST state must be incorporated into any of the zero states, in order to avoid any impact on the active states. Consequently, on the output AC voltage.

The traditional PWM techniques used for the conventional inverter are not adapted to the qZSI. In fact, several modified PWM are used for controlling the qZSI. Therefore, miscellaneous PWM techniques have been proposed in the literature, which can be broadly categorized into two distinct methods, namely, sinusoidal PWM (SPWM) and SVM. Among the SPWM techniques are the simple boost, maximum boost [13], and maximum constant boost [14], which were the first methods introduced. The conventional space vector modulation (SVPWM) technique has gained widespread popularity due to its ability to produce a high DC voltage with reduced harmonic distortion. Owing to these benefits, the concept of SVPWM has been extended to control the qZSI [15].

The conventional VSI is commonly operated using the traditional SVPWM technique. This technique uses eight voltage space states, which consist of six active states and two zero states, resulting in the generation of six sectors as it is shown in Figure 6. The modified SVPWM are commonly called ZSVM. According to [15], the ZSVM used for qZSI employs six active vectors, two zero vectors, and an additional shoot-through (ST) vector. The reference output voltage can be expressed in (7):

$$Uref = \frac{T_1}{T_s}U_1 + \frac{T_2}{T_s}U_2 + \frac{T_0 - T_{sh}}{T_s}U_0 + \frac{T_{sh}}{T_s}U_{sh} \qquad (7)$$

where:

$$\begin{cases} T_1 = T_s M \sin(\frac{\pi}{3}i - \theta) \\ T_2 = T_s M \sin(\theta - \frac{\pi}{3}(i-1)) \end{cases} and \begin{cases} T_0 = T_s - T_1 - T_2, \ T_{sh} = DT_s \\ M = \sqrt{3}\frac{U_{ref}}{V_{dc}} \end{cases}$$

Where, i denotes i^{th} sector (1 to 6), T_0 is the time interval of zero vector U_0, U_{sh} is the vector of the ST state, T_1 and T_2 are the duration of active vectors U_1 and U_2, respectively, and θ is the angle between U_{ref} and U_1 as shown in Figure 6. M is the modulation index.

The ST state is incorporated during the time intervals of the zero state. It is pertinent to note that the active state remains unaffected and maintains its state as in conventional SVM. The total duration of the ST state T_{sh} involves the use of the desired duty cycle ratio D. Subsequently, the T_{sh} is divided into several segments per switching cycle [15]. Each of these segments is independently introduced between the active state vector and the zero-state vector.
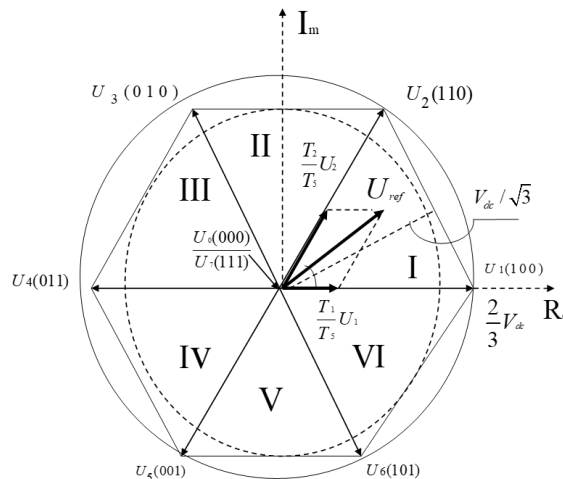
Figure 6. SVPWM vectors and generated sectors I

According to the number of parts on which the total ST time is divided and the way of their placement during the switching cycle. Three variants of ZSVM have been described in the literature, namely ZSVM6, ZSVM4, and ZSVM2. The theoretical details, as well as the characteristics and limitations of each technique have been extensively discussed in [15].

Based on the in-depth discussion presented in [15], the current work has adopted ZSVM4 due to its perceived advantages over other variants. The ZSVM4 technique involves dividing the total ST time T_{sh} into six parts, which are inserted according to the schematic representation presented in Figure 7. Compared to the conventional SVM, ZSVM4 requires the modification of four switching control signals. Therefore, the suffix "4" is added to its name to indicate this distinction.

Figure 7. Switching time of ZSVM4 in sector I

For a reference vector U_{ref} that belongs to sector I, the Figure 7 presents switching control signals. A similar analysis is employed for the other sectors to determine their corresponding switching patterns by using the mathematical expressions provided in (8) and (9).

$$T \frac{T_0}{4}_{mid} \quad \frac{T_0}{4} \frac{T_1}{2} \frac{T_0}{4} \frac{T_1}{2} \frac{T_2}{2}_{max}{}_{min} \tag{8}$$

$$\begin{cases} T_{min+} = T_{min+} - \frac{T_{sh}}{6} \\ T_{min-} = T_{min} \end{cases} \begin{cases} T_{mid+} = T_{mid} \\ T_{mid-} = T_{mid} + \frac{T_{sh}}{6} \end{cases} \begin{cases} T_{max+} = T\frac{T_{sh}}{6}{}_{max} \\ T_{max-} = T\frac{T_{sh}}{3}{}_{max} \end{cases} \tag{9}$$

2.2.4. Control schemes for the grid connected

The control system for the grid-connected qZSI in PV systems is not similar to the constant DC input source qZSI system. The control structure of the system comprises two primary stages. The first stage is the DC-side control, The primary function of this step is to regulate the DC-link voltage. Whereas, the

second stage is the AC-side control, which is composed of two cascaded controller loops. Specifically, the system includes ZSVM block, phase locking loop (PLL), Clark transformation from abc to αβ, and park transformation from dq to $\alpha\beta$. These components are essential for the system to operate effectively and produce the desired output.

a. DC side voltage control

On the DC-side control, a dual-loop PI-based control scheme is employed to effectively maintain a constant peak DC-link voltage at the desired value. As depicted in Figure 3, the control scheme uses the adjustment of the voltage across the capacitor (V_{C1}) and the inductor current (i_L) to generate the shoot-through duty ratio D.

In order to ensure the appropriate regulation of voltage V_{dc}, it becomes necessary to compare its actual value with the desired value. However, due to the pulsating nature of V_{dc}, the measurement of its actual value calls for the utilization of specialized and expensive circuitry. Therefore, to address this challenge, the indirect V_{dc} control method is employed, wherein the estimation of V_{dc} is derived from the measurement of V_{C1} using the formula specified in (5) and (6).

As it is shown in Figure 3, the error between the desired value V_{dc}^* and the actual value V_{dc} is processed through a PI regulator. This regulator serves to furnish the reference current i_L^* for the inner loop's inductor. Subsequently, another PI regulator utilizes the error between i_L^* and the present inductor current i_L to generate the shoot-through duty cycle D.

b. AC side power control

In the proposed control scheme, the AC side control is similar to a voltage VSI, the qZSI assumes the responsibility of regulating both the active and reactive power through the modulation index M. In order to address the objective of AC side control, a d-q reference frame aligned with the grid voltage is employed to achieve the decoupling of active and reactive power control. In fact, the currents and voltages of the three-phase grid are measured and subsequently converted into d-q components. Additionally, the three-phase AC voltages undergo routing through a phase locking loop to obtain the three-phase voltage phases.

To accomplish the decoupling of active and reactive power control, two cascaded control loops are employed to regulate these powers. The outer loop serves the purpose of power control, while the inner loop is employed for current regulation. The imposition of the reactive power reference is conducted externally, while the active power is contingent upon the power extracted from the photovoltaic panel. As expected in Figure 3, the MPPT algorithm is used to determine the reference for the d-axis of the current (i_d) injected into the grid, while a value of zero is enforced on the q-axis current (i_q) component reference.

For the inner loop, two feedback controls are implemented to regulate i_d and i_q individually, due to the contribution of the decoupling terms as shown in Figure 8. Each of these controls utilizes PI regulators to accurately track their respective current references. The resulting output variables from these controllers are the compensation terms (voltage references) v_d^* and v_q^*. By employing the dq/abc transformation, the voltage references for the inverter output can be derived v_a^*, v_b^* and v_c^*. Finally, these voltage references and duty ratio cycle (derived from DC side control) are subsequently employed in ZSVM algorithm to generate the gate PWM signals required to drive the inverter.
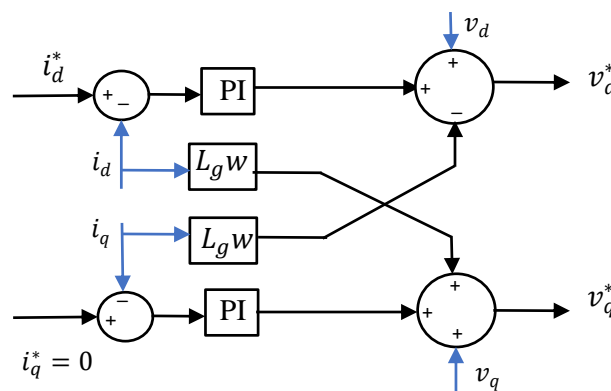
Figure 8. AC-side control decoupling terms

3. RESULTS AND DISCUSSION

The proposed structure depicted in Figure 3 was implemented using MATLAB/Simulink and PLECS. The operation and control of the proposed control scheme for the qZSI in a PV system are simulated. Various irradiation levels are taken into account during the simulation to assess the system's performance under different solar intensity conditions. The achieved outcomes are presented in this section.

3.1. Simulation specifications

To evaluate the performance and effectiveness of the proposed control system, a trapezoidal solar irradiation profile is applied to the PV generator while assuming a constant cell temperature. The solar irradiation level is depicted in Figure 9. Initially, from 0 to 6 s, the irradiation level is set at 500 W/m^2. Subsequently, it progressively increases in a linear manner, reaching 800 W/m^2 between 6 and 12.5 s. Finally, it decreases linearly back to 500 W/m^2. The solar panel specifications used in this study is shown in Table 1 while the Table 2 illustrates the main designed parameters of the grid-connected qZSI system.
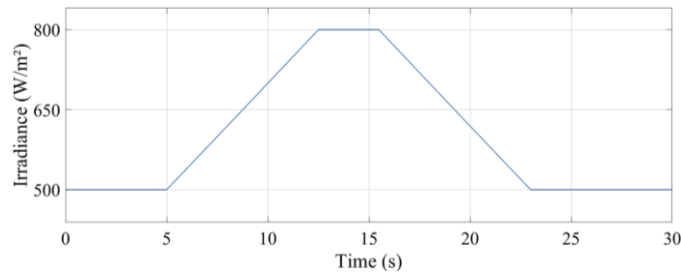
Figure 9. Applied irradiance profile

Table 1. PV generator specifications

PV generator parameters	Values
Maximum power P_{MPP}	288 W
V_{MPP}	162 V
I_{MPP}	1.93 A
v_{oc}	200 V
capacitor value at PV generator terminals C_{PV}	500 µF

Table 2. Designed parameters of the grid-connected qZSI system

qZSI and grid parameters	Values
Maximum voltage at grid terminals	100 V
Grid frequency	50 Hz
Switching frequency	10 kHz
Grid filter	$Lg = 2\ mH\ ; Rg = 0.5\ \Omega$
Impedance network	$C = C_1 = C_2 = 200$ µF
	$L = L_1 = L_2 = 50$ µH
DC-link voltage reference	200 V

3.2. Simulation results and discussion

Both the power effectively extracted from the PV generator and its maximum power is presented in Figure 10. It is evident from the plot that during steady-state conditions, the PV output power aligns closely with the maximum power. It can be inferred that Figure 10 demonstrates the effective control of active power in response to changes in irradiance.

Figure 11 displays the simulation results showing the injected current and grid voltage. In Figure 11(a) the grid's injected current and grid voltage are depicted across the entire simulation duration, whereas Figure 11(b) shows a zoomed-in area of the current and grid voltage. From Figure 11(b) it can be seen that the grid current and voltage are in phase, indicating that the system operates at a unity power factor. In addition, the grid current exhibits significantly reduced harmonics due to eliminating the dead-time between the upper and lower devices within a single phase-leg. Without forgetting the impact of the implementation of SVM technique over the harmonics. On the other hand, we can conclude from Figure 12 that the PV output voltage (Vpv) closely tracks the MPPT reference voltage ($Vref$) which progressively converges towards the voltage V_{mpp} associated with MPP operation.
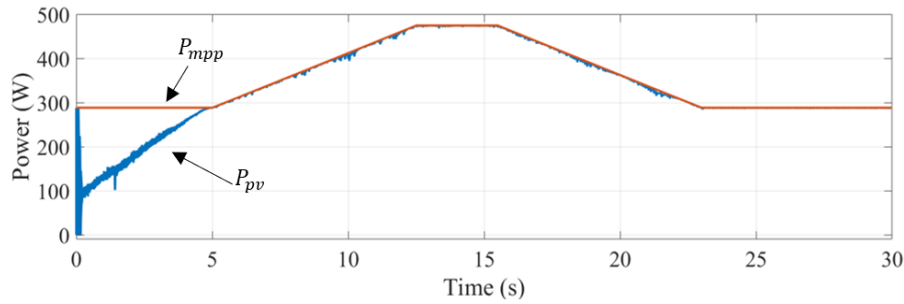
Figure 10. Simulation results, PV output power

(a)

(b)
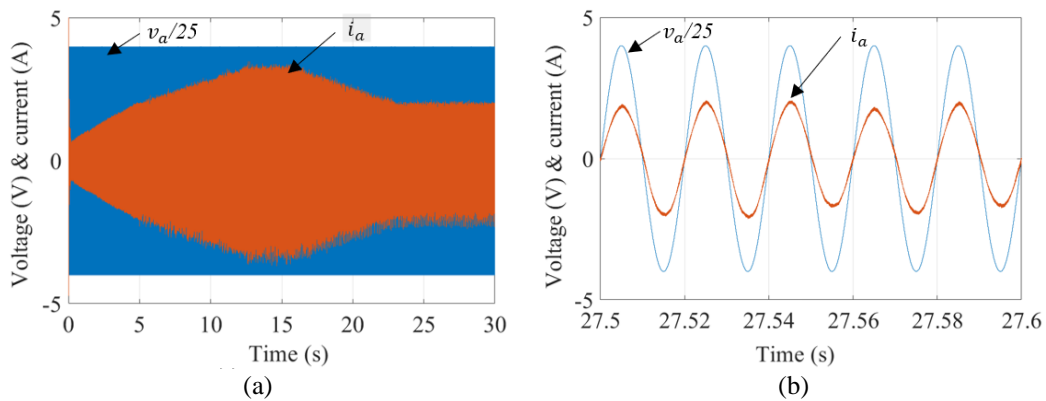
Figure 11. Simulation results (a) grid i_a current and grid voltage v_a and (b) zoomed-in area of i_a and v_a
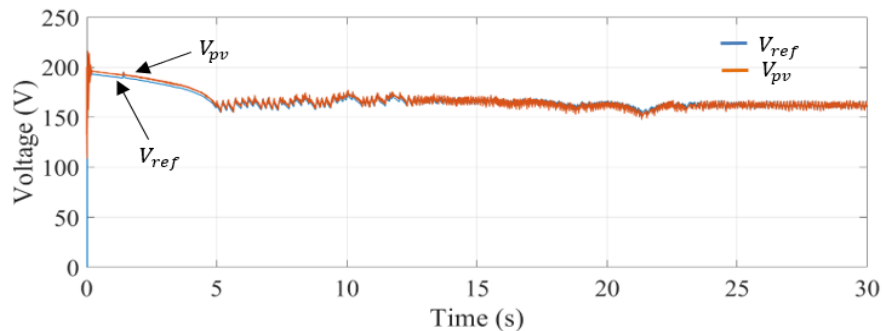
Figure 12. Simulation results MPPT reference voltage ($Vref$) and PV output voltage (Vpv)

On the subject of the DC-link voltage, Figure 13 illustrates the simulation results for both the DC-link voltage and the ST duty ratio. it is possible to observe from Figure 13 that the voltage is effectively regulated at the predetermined set value 200 V. Indeed, the change of the irradiance has no apparent impact on the peak DC-link voltage which is almost the same as it shown in Figure 13(a).

The oscillation of the PV output voltage during the MPP search results in oscillations of the ST duty ratio, as it presented in Figure 13(b) which ensures the stability of the DC-link voltage. Otherwise, in the steady-state of the PV output voltage, it is evident that the ST duty ratio remains stable and confirming the relationship between PV output voltage and DC-link voltage as presented in (6). Based on the aforementioned results and a comparison with the findings reported in [10], [21]–[23], [27], it is evident that the proposed control strategy effectively achieves maximum power extraction from the PV generator while simultaneously regulating the DC-link voltage and ensuring unity power factor operation. On other hand the proposed control strategy extracts maximum power while exhibiting fewer steady-state oscillations compared to the method proposed in [23], [26].
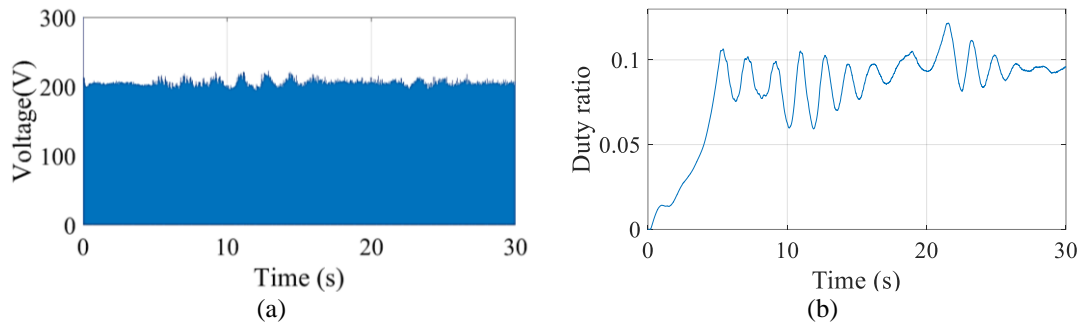
Figure 13. Simulation results (a) DC-link voltage and (b) shoot-through duty ratio

4. CONCLUSION

The qZSI used for grid connected PV applications are studied in this paper. A decoupled control scheme is proposed based on the MPPT algorithm, ZSVM technique and PI controllers. The main objective of proposed scheme control is to harvest the maximum power from the PV, regulating DC-link voltage and monitoring the power factor of the grid. The operating principle and modeling of qZSI are firstly presented, then the proposed scheme control is described and analyzed. The decoupled control law successfully drove the qZSI to inject three-phase current into the grid, presenting excellent synchronization and achieving a low total THD of 5%. While the results obtained are satisfactory, there is still potential for improvement in the control strategy. The use of an adaptive step MPPT P&O technique can enhance the response time and mitigate steady-state power oscillations. In parallel with ongoing efforts to improve the proposed control strategy, the next step is the experimental realization by implementation on a platform consisting of a dSPACE electronic board and the RTbox simulator.

REFERENCES

[1]   S. Kouro, J. I. Leon, D. Vinnikov, and L. G. Franquelo, "Grid-connected photovoltaic systems: an overview of recent research and emerging PV converter technology," *IEEE Industrial Electronics Magazine*, vol. 9, no. 1, pp. 47–61, Mar. 2015, doi: 10.1109/MIE.2014.2376976.
[2]   Y. Liu, H. Abu-Rub, B. Ge, F. Blaabjerg, O. Ellabban, and P. C. Loh, *Impedance source power electronic converters*. Wiley, 2016.
[3]   A. Loubna, T. Riad, and M. Salima, "Standalone photovoltaic array fed induction motor driven water pumping system," *International Journal of Electrical and Computer Engineering (IJECE)*, vol. 10, no. 5, pp. 4534–4542, Oct. 2020, doi: 10.11591/ijece.v10i5.pp4534-4542.
[4]   H. S. Kamil, D. M. Said, M. W. Mustafa, M. R. Miveh, and N. Ahmad, "Low-voltage ride-through for a three-phase four-leg photovoltaic system using SRFPI control strategy," *International Journal of Electrical and Computer Engineering (IJECE)*, vol. 9, no. 3, pp. 1524–1530, Jun. 2019, doi: 10.11591/ijece.v9i3.pp1524-1530.
[5]   M. Moutchou and A. Jbari, "Fast photovoltaic IncCond-MPPT and backstepping control, using DC-DC boost converter," *International Journal of Electrical and Computer Engineering (IJECE)*, vol. 10, no. 1, pp. 1101–1112, Feb. 2020, doi: 10.11591/ijece.v10i1.pp1101-1112.
[6]   F. Z. Peng, "Z-source inverter," *IEEE Transactions on Industry Applications*, vol. 39, no. 2, pp. 504–510, Mar. 2003, doi: 10.1109/TIA.2003.808920.
[7]   Y. P. Siwakoti, F. Z. Peng, F. Blaabjerg, P. C. Loh, and G. E. Town, "Impedance-source networks for electric power conversion Part I: A topological review," *IEEE Transactions on Power Electronics*, vol. 30, no. 2, pp. 699–716, Feb. 2015, doi: 10.1109/TPEL.2014.2313746.
[8]   I. Jamal, M. F. Elmorshedy, S. M. Dabour, E. M. Rashad, W. Xu, and D. J. Almakhles, "A comprehensive review of grid-connected PV systems based on impedance source inverter," *IEEE Access*, vol. 10, pp. 89101–89123, 2022, doi: 10.1109/ACCESS.2022.3200681.
[9]   J. Anderson and F. Z. Peng, "A class of quasi-z-source inverters," in *2008 IEEE Industry Applications Society Annual Meeting*, Oct. 2008, pp. 1–7, doi: 10.1109/08IAS.2008.301.
[10] Y. Li, F. Z. Peng, J. G. Cintron-Rivera, and S. Jiang, "Controller design for quasi-Z-source inverter in photovoltaic systems," in *2010 IEEE Energy Conversion Congress and Exposition*, Sep. 2010, pp. 3187–3194, doi: 10.1109/ECCE.2010.5618288.
[11] Y. Li, S. Jiang, J. G. Cintron-Rivera, and F. Z. Peng, "Modeling and control of quasi-Z-source inverter for distributed generation applications," *IEEE Transactions on Industrial Electronics*, vol. 60, no. 4, pp. 1532–1541, Apr. 2013, doi: 10.1109/TIE.2012.2213551.
[12] E. P. P. Soares-Ramos, L. De Oliveira-Assis, R. Sarrias-Mena, P. Garcia-Trivino, C. A. Garcia-Vazquez, and L. M. Fernandez-Ramirez, "Averaged dynamic modeling and control of a quasi-Z-source inverter for wind power applications," *IEEE Access*, vol. 9, pp. 114348–114358, 2021, doi: 10.1109/ACCESS.2021.3104797.
[13] F. Z. Peng, M. Shen, and Z. Qian, "Maximum boost control of the Z-source inverter," *IEEE Transactions on Power Electronics*, vol. 20, no. 4, pp. 833–838, Jul. 2005, doi: 10.1109/TPEL.2005.850927.
[14] M. Shen, J. Wang, A. Joseph, F. Z. Peng, L. M. Tolbert, and D. J. Adams, "Maximum constant boost control of the Z-source inverter," in *Conference Record of the 2004 IEEE Industry Applications Conference, 2004. 39th IAS Annual Meeting.*, 2004, vol. 1, pp. 142–147, doi: 10.1109/IAS.2004.1348400.

[15] Y. Liu, B. Ge, H. Abu-Rub, and F. Z. Peng, "Overview of space vector modulations for three-phase Z-source/quasi-z-source inverters," *IEEE Transactions on Power Electronics*, vol. 29, no. 4, pp. 2098–2108, Apr. 2014, doi: 10.1109/TPEL.2013.2269539.

[16] L. Monjo, L. Sainz, J. J. Mesas, and J. Pedra, "State-space model of quasi-Z-source inverter-PV systems for transient dynamics studies and network stability assessment," *Energies*, vol. 14, no. 14, Jul. 2021, doi: 10.3390/en14144150.

[17] V. Castiglia, R. Miceli, F. Blaabjerg, and Y. Yang, "Small-signal modeling and experimental validation of the three-phase quasi-Z-source inverter," in *2020 IEEE 21st Workshop on Control and Modeling for Power Electronics (COMPEL)*, Nov. 2020, pp. 1–8, doi: 10.1109/COMPEL49091.2020.9265716.

[18] E. Jaoide, F. El Aamri, M. Outazkrit, A. Radouane, and A. Mouhsen, "Characteristics dynamic analysis and modeling of quasi-Z-source inverters for PV applications," in *The Proceedings of the International Conference on Electrical Systems and Automation*, Singapore: Springer Singapore, 2022, pp. 91–102.

[19] W. Liu, Y. Yang, T. Kerekes, E. Liivik, and F. Blaabjerg, "Impedance network impact on the controller design of the QZSI for PV applications," in *2020 IEEE 21st Workshop on Control and Modeling for Power Electronics (COMPEL)*, Nov. 2020, pp. 1–6, doi: 10.1109/COMPEL49091.2020.9265708.

[20] A. Sangari, R. Umamaheswari, M. G. Umamaheswari, and L. Sree B, "A novel SOSMC based SVPWM control of Z-source inverter for AC microgrid applications," *Microprocessors and Microsystems*, vol. 75, Jun. 2020, doi: 10.1016/j.micpro.2020.103045.

[21] F. Bagheri, H. Komurcugil, O. Kukrer, N. Guler, and S. Bayhan, "Multi-input multi-output-based sliding-mode controller for single-phase quasi-Z-source inverters," *IEEE Transactions on Industrial Electronics*, vol. 67, no. 8, pp. 6439–6449, Aug. 2020, doi: 10.1109/TIE.2019.2938494.

[22] T. Hou, C.-Y. Zhang, and H.-X. Niu, "Quasi-Z source inverter control of PV grid-connected based on fuzzy PCI," *Journal of Electronic Science and Technology*, vol. 19, no. 3, Sep. 2021, doi: 10.1016/j.jnlest.2020.100021.

[23] N. Singh and S. K. Jain, "TOIL and damped-SOGI control of quasi-Z-source inverter based grid-connected renewable-system," *Control Engineering Practice*, vol. 90, pp. 267–284, Sep. 2019, doi: 10.1016/j.conengprac.2019.07.004.

[24] D. Ma, K. Cheng, R. Wang, S. Lin, and X. Xie, "The decoupled active/reactive power predictive control of quasi-Z-source inverter for distributed generations," *International Journal of Control, Automation and Systems*, vol. 19, no. 2, pp. 810–822, Feb. 2021, doi: 10.1007/s12555-019-0698-9.

[25] S. Vadi and R. Bayindir, "Modeling, analysis and proportional resonant and proportional integral based control strategy for single phase quasi-Z source inverters," *IEEE Access*, vol. 10, pp. 87217–87226, 2022, doi: 10.1109/ACCESS.2022.3199732.

[26] Y. Liu, H. Abu-Rub, B. Ge, F. Peng, A. T. de Almeida, and F. J. T. E. Ferreira, "An improved MPPT method for quasi-Z-source inverter based grid-connected photovoltaic power system," in *2012 IEEE International Symposium on Industrial Electronics*, May 2012, pp. 1754–1758, doi: 10.1109/ISIE.2012.6237356.

[27] W. Liu, Y. Yang, and T. Kerekes, "Characteristic analysis of the grid-connected impedance-source inverter for PV applications," in *2019 IEEE 10th International Symposium on Power Electronics for Distributed Generation Systems (PEDG)*, Jun. 2019, pp. 874–880, doi: 10.1109/PEDG.2019.8807487.

[28] E. Jaoide, F. El Aamri, M. Outazkrit, A. Radouane, and A. Mouhsen, "PI-based ZSVM control of quasi-Z-source inverter for photovoltaic applications in standalone mode," *Indonesian Journal of Electrical Engineering and Informatics (IJEEI)*, vol. 11, no. 1, pp. 50–60, Feb. 2023, doi: 10.52549/ijeei.v11i1.4224.

[29] M. Sarvi and A. Azadian, "A comprehensive review and classified comparison of MPPT algorithms in PV systems," *Energy Systems*, vol. 13, no. 2, pp. 281–320, May 2022, doi: 10.1007/s12667-021-00427-x.

[30] N. Jaalam, N. A. Rahim, A. H. A. Bakar, C. Tan, and A. M. A. Haidar, "A comprehensive review of synchronization methods for grid-connected converters of renewable energy source," *Renewable and Sustainable Energy Reviews*, vol. 59, pp. 1471–1481, Jun. 2016, doi: 10.1016/j.rser.2016.01.066.

BIOGRAPHIES OF AUTHORS

Essaid Jaoide 🆔 📇 SC 🔾 was born in 27 January 1990 in Beni Mellal, Morocco. He is a Ph.D. student in Laboratory of Radiation-Matter and Instrumentation (RMI), Faculty of Sciences and Technology, Hassan 1st University, Morocco. he received his Master degree in electrical engineering from Cadi Ayyad University Marrakech, in 2013. He also obtained the Agrégation degree in Electrical Engineering in 2018. His researches are in fields impedance source power electronic converters and grid-connected photovoltaic systems. He can be contacted at email: e.jaoide@uhp.ac.ma.

Faicel El Aamri 🆔 📇 SC 🔾 received his Ph.D. on PV systems from Hassan first University in 2018. He currently works as Professor at Hassan II University, Faculty of Sciences and technologies of Mohammedia, Morocco. His area of research interest is the control of Grid-connected PV inverters and power electronics. He can be contacted at email: f.elaamri@gmail.com.

Mbarek Outazkrit received the M.S. degree in electrical engineering from Cadi Ayyad University in 2014. He also obtained the Aggregation degree in electrical engineering in 2016. Mbarek works in Ph.D. at Ph.D. Center of physics and engineering sciences in Hassan First University. His area of interest is modular multilevel converters MMC, power converter applications in power systems, grid integration of renewable energy sources. He can be contacted at email: m.outazkrit@uhp.ac.ma.

Abdelhadi Radouane was born in 1969. He received the Aggregation degree in electrical engineering from the ENSET of Rabat, Morocco in 1996. In 2017, he obtained a Ph.D. in automatic control. Since 2018, he joined the FST Settat, Hassan First University of Settat, Morocco as assistant-professor. He can be contacted at email: radouane.abdelhadi@gmail.com.

Azeddine Mouhsen was born in 10 July 1967, he is professor of physics at Hassan First University, Morocco, since 1996. He holds a Ph.D. from Bordeaux I University (France) in 1995 and a thesis from Moulay Ismail University, Morocco, in 2001. He specializes in instrumentation and measurements, sensors, applied optics, energy transfer, radiation-matter interactions. He has taught courses in physical sensors, chemical sensors, instrumentation, systems technology, digital electronics and industrial data processing. He has published over 30 papers and he is the co-inventor of one patent. Actually, he is the Director of Laboratory of radiation-matter and Instrumentation. He can be contacted at email: az.mouhsen@gmail.com.